

7. Keil, R. G., Tsamakis, E., Fuh, C. B., Giddings, J. C. & Hedges, J. I. *Geochim. cosmochim. Acta* **58**, 879–893 (1994).
8. Mayer, L. M. *Geochim. cosmochim. Acta* **58**, 1271–1284 (1994).
9. Eglinton, G. in *Organic Geochemistry* (eds Eglinton, G. & Murphy, M. T. J.) 20–71 (Springer, New York, 1969).
10. Henrichs, S. M. & Sugai, S. F. *Geochim. cosmochim. Acta* **57**, 823–835 (1993).
11. Pinck, L. A. & Allison, F. E. *Science* **114**, 130–131 (1951).
12. Wang, X.-C. & Lee, C. *Mar. Chem.* **44**, 1–24 (1993).
13. Marshman, N. A. & Marshall, K. C. *Soil Biol. Biochem.* **13**, 127–134 (1981).
14. Ogram, A. V. et al. *Appl. envir. Microbiol.* **49**, 582–587 (1985).
15. van Loosdrecht, M. C. M. et al. *Microbiol. Rev.* **54**, 75–87 (1990).
16. Doyle, L. J. & Garrels, R. M. *Geo-Mar. Lett.* **5**, 51–53 (1985).
17. Berner, R. A. *Am. J. Sci.* **291**, 339–376 (1991).
18. Keil, R. G. & Kirchman, D. L. *Mar. Ecol. Prog. Ser.* **73**, 1–10 (1991).

ACKNOWLEDGEMENTS. We appreciate comments provided by R. Benner, M. Peterson, B. Bergamaschi and the UW Marine Organic Geochemistry group; L. Mayer provided encouragement and stimulating discussions. We thank E. Tsamakis, K. Rossner and C. Cooper for technical support, and Chih-An Huh from OSU for graciously providing the  $^{210}\text{Pb}$  data. This research was supported by the US NSF.

## Archaean crustal development in the Lewisian complex of northwest Scotland

Kevin W. Burton\*, Anthony S. Cohen\*,  
R. Keith O'Nions\* & Michael J. O'Hara†

\* Department of Earth Sciences, University of Cambridge,  
Downing Street, Cambridge CB2 3EQ, UK

† Department of Geology, University of Cardiff, Cardiff CF1 3YG, UK

THE Lewisian complex of northwest Scotland is typical of many Archaean terrains and has a well documented history starting ~2,700 Myr ago<sup>1–6</sup>. Here we present new isotopic data that extend this history back to 3,300 Myr, and provide some insight into how the earliest continental crust may have formed. The Lewisian is dominated by tonalite, trondhjemite and granodiorite (TTG) rocks, which require a mafic lithospheric source, rather than being direct mantle melts<sup>7–11</sup>. But the mafic and ultramafic rocks in the high-grade granulite-facies part of this terrain show little evidence of a significantly older crustal history<sup>12,13</sup> and precursor material to the TTG lithologies has not yet been identified. Here we show that older amphibolite material has survived at a lower metamorphic grade. Coexisting amphibolite minerals yield indistinguishable  $^{207}\text{Pb}$ – $^{206}\text{Pb}$  and  $^{147}\text{Sm}$ – $^{143}\text{Nd}$  ages of  $3,310 \pm 27$  Myr and  $3,298 \pm 73$  Myr, respectively. These data are consistent with an origin for much of the Lewisian terrain by the re-melting of pre-existing lithosphere, with an isotopic signature similar to that of the amphibolites studied here.

Low-grade amphibolite-facies rocks in the Lewisian terrain occur at Gruinard Bay. Layered amphibolites and tonalites at this locality are intruded by trondhjemitic gneiss, forming a large-scale agmatite complex<sup>14,15</sup>. Field relationships suggest that these amphibolites are one of the earliest parts of the Lewisian complex, and trace-element chemistry suggests that they are a potential source for many of the TTG rock types<sup>14,15</sup>. Thus it is possible that they preserve valuable information on crustal evolution in this terrain. We have obtained samarium–neodymium and lead isotopic data for the amphibolite and trondhjemite mineral assemblages from Gruinard Bay, and compare our results with those of earlier studies of TTG lithologies in this terrain<sup>1–6</sup>.

Chemical and isotopic data for mineral and whole-rock separates taken from both trondhjemite and amphibolite samples are given in Table 1 (see legend for details of mineral petrography). Analytical procedures follow those reported previously<sup>16</sup>. For the trondhjemites both  $^{207}\text{Pb}$ – $^{206}\text{Pb}$  and  $^{147}\text{Sm}$ – $^{143}\text{Nd}$  ages are in good agreement and indicate that equilibration of Sm–Nd and Pb between minerals occurred ~2,400 Myr ago

(Table 2). In contrast, Pb isotopic data for whole-rock and mineral separates from the amphibolite samples yields  $^{207}\text{Pb}$ – $^{206}\text{Pb}$  versus  $^{206}\text{Pb}$ – $^{204}\text{Pb}$  regression ages of  $3,310 \pm 26$  Myr and  $3,314 \pm 61$  Myr, respectively (Fig. 1a; Table 2). Sm–Nd data for sample GR102 give an age of  $3,298 \pm 73$  Myr (Fig. 1b; Table 2). The Sm–Nd results for sample GR11 yield no meaningful age information, and these data are most probably biased by the presence of retrograde phases. Both  $^{207}\text{Pb}$ – $^{206}\text{Pb}$  ages, and the  $^{147}\text{Sm}$ – $^{143}\text{Nd}$  age for sample GR102, indicate that the mineral equilibration in the amphibolites occurred ~3,300 Myr ago. This

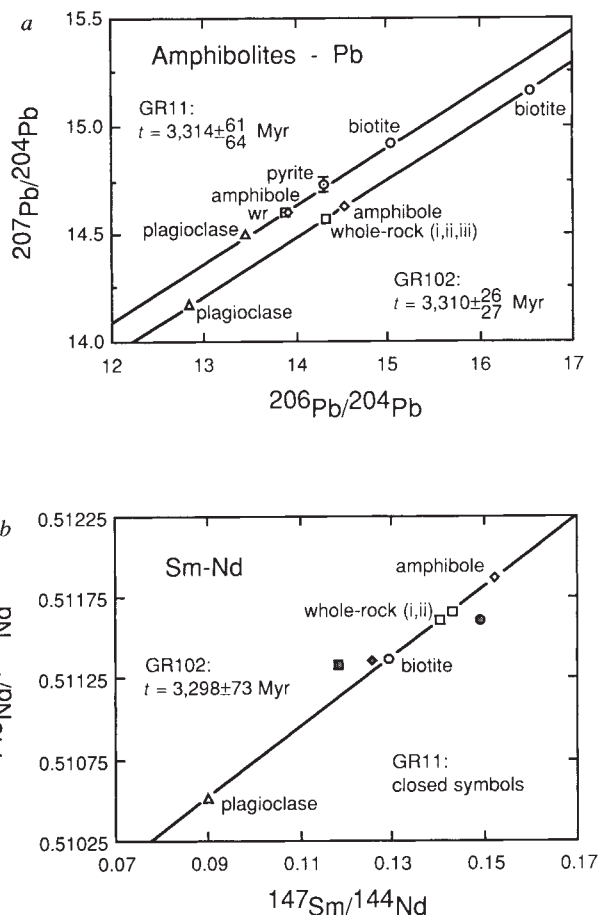


FIG. 1 a,  $^{207}\text{Pb}$ – $^{206}\text{Pb}$  evolution diagram for amphibole (diamonds), biotite (circles), plagioclase (triangles), pyrite (dotted circle) and whole-rock (squares) separates from the amphibolite samples (GR102 and GR11) from Gruinard Bay. The data for sample GR102 yield a best-fit line corresponding to an age of  $3,310 \pm 26$  Myr; mean-square weighted deviation is 0.78. Sample GR11 gives an age of  $3,314 \pm 61$  Myr; mean-square weighted deviation is 4.25. b,  $^{147}\text{Sm}$ – $^{143}\text{Nd}$  evolution diagram for the minerals shown in Fig. 2a. The data for sample GR102 yield a best-fit line corresponding to an age of  $3,298 \pm 73$  Myr; mean-square weighted deviation is 0.27. Data from sample GR11 (filled symbols) are also shown, but do not yield any meaningful age information. The age obtained for sample GR102 is in excellent agreement with the  $^{207}\text{Pb}$ – $^{206}\text{Pb}$  data from both amphibolite samples, and indicate that equilibration of both Sm–Nd and Pb between minerals in the amphibolites occurred 3,300 Myr ago. This age is ~600 Myr older than the time of depletion in the higher-grade granulites<sup>1–6</sup>, and 900 Myr older than the minerals in the adjacent trondhjemites. (Note that the statistical precision of all of the isochrons both here and in Table 2 is excellent; however, all of the phases analysed have low U/Pb and Sm/Nd ratios. Under these circumstances the relatively large uncertainties in the age estimates arise as a result of the small amount of ingrowth of radiogenic Pb and Nd, rather than owing to analytical errors or geological disturbance.)

TABLE 1 Isotope data for trondhjemites and amphibolites at Gruinard Bay

Whole-rock/ mineral	$^{206}\text{Pb}/^{204}\text{Pb}^*$	$^{207}\text{Pb}/^{204}\text{Pb}^*$	$^{208}\text{Pb}/^{204}\text{Pb}^*$	$^{143}\text{Nd}/^{144}\text{Nd}^\dagger$	$^{147}\text{Sm}/^{144}\text{Nd}^\ddagger$	[Pb] (p.p.m. by wt)	[Sm] (p.p.m. by wt)	[Nd] (p.p.m. by wt)
<b>Trondhjemites</b>								
<b>GR100</b>								
Whole-rock	14.187 ± 0.014	14.595 ± 0.016	34.326 ± 0.038	0.511102 ± 26	0.1124	8.831	0.7261	3.904
Amphibole	15.791 ± 0.014	14.865 ± 0.016	38.242 ± 0.032	0.511777 ± 20	0.1548	2.208	1.353	5.284
Biotite	16.623 ± 0.016	14.993 ± 0.018	37.542 ± 0.034	0.511246 ± 20	0.1201	2.770	0.6087	3.063
Plagioclase	13.910 ± 0.010	14.578 ± 0.016	33.969 ± 0.028	0.511000 ± 26	0.1055	7.286	0.2972	1.703
<b>GR103</b>								
Whole-rock	13.628 ± 0.012	14.525 ± 0.016	35.559 ± 0.034	0.511170 ± 18	0.1138	9.508	4.868	25.86
Amphibole	14.561 ± 0.012	14.679 ± 0.016	36.933 ± 0.032	0.511871 ± 14	0.1591	2.757	9.720	36.92
Plagioclase	13.489 ± 0.010	14.496 ± 0.010	34.686 ± 0.026	0.510635 ± 20	0.0802	7.892	0.4862	3.664
<b>Amphibolites</b>								
<b>GR102</b>								
Whole-rock i§	14.321 ± 0.016	14.573 ± 0.016	37.096 ± 0.038	0.511604 ± 20	0.1401	1.930	11.58	49.97
Whole-rock ii§	14.324 ± 0.018	14.564 ± 0.018	36.929 ± 0.044	0.511661 ± 18	0.1430	1.924	11.77	49.75
Whole-rock iii	14.317 ± 0.012	14.566 ± 0.018	36.988 ± 0.036	—	—	1.578	—	—
Amphibole	14.544 ± 0.016	14.624 ± 0.016	36.796 ± 0.044	0.511873 ± 14	0.1524	2.551	17.07	67.72
Biotite	16.536 ± 0.016	15.172 ± 0.016	37.440 ± 0.038	0.511374 ± 20	0.1293	1.303	3.880	18.13
Plagioclase	12.855 ± 0.010	14.177 ± 0.016	35.220 ± 0.028	0.510511 ± 26	0.0901	2.706	1.341	8.991
<b>GR11</b>								
Whole-rock	13.897 ± 0.010	14.594 ± 0.016	37.177 ± 0.038	0.511330 ± 6	0.1182	1.221	4.927	25.18
Amphibole	13.912 ± 0.010	14.594 ± 0.016	36.683 ± 0.028	0.511360 ± 6	0.1259	1.714	14.04	67.37
Biotite	15.047 ± 0.010	14.919 ± 0.016	36.083 ± 0.028	0.511613 ± 8	0.1490	0.9732	1.336	5.419
Plagioclase	13.462 ± 0.010	14.498 ± 0.016	34.884 ± 0.028	—	—	2.339	—	—
Pyrite	14.297 ± 0.036	14.730 ± 0.036	36.241 ± 0.094	—	—	—	—	—

All quoted errors are  $2\sigma_m$ . Maximum procedural blanks are 60 pg for Pb, 5 pg for Nd and 2 pg for Sm.

All samples were taken from a large roadcut on the west side of Gruinard Bay (grid reference: NG941902). The trondhjemite mineral assemblage comprises plagioclase( $\text{An}_{25}$ )–quartz–hornblende–biotite–epidote–apatite–sphene. The amphibolite mineral assemblage consists of hornblende–biotite–plagioclase( $\text{An}_{19}$ )–calcite–clinozoisite–ilmenite( $X_{\text{ilm}} = 0.943$ )–magnetite( $X_{\text{usp}} = 0.006$ )–pyrite. (Electron microprobe analyses for the major mineral phases are available on request from K.W.B.) In the amphibolites studied here the original high-Ti pargasitic hornblende has been pseudomorphed by edenite with exsolved ilmenite; more rarely, hornblende shows sieve-textured quartz inclusions considered to be retrograde after clinopyroxene. Amphibolite GR11 shows extensive alteration and contains calcite, scapolite, alkali feldspar, chlorite and Fe–Ti oxides rimmed by sphene. The trondhjemites also show evidence of retrogression, with hornblende after clinopyroxene. Plagioclase in both rock types is sometimes altered to sericite, clinozoisite and muscovite.

\* Pb isotope ratios relative to NBS981 standard, which yields  $^{206}\text{Pb}/^{204}\text{Pb} = 16.932 \pm 0.012$ ,  $^{207}\text{Pb}/^{204}\text{Pb} = 15.486 \pm 0.016$ ,  $^{208}\text{Pb}/^{204}\text{Pb} = 36.691 \pm 0.036$  ( $2\sigma$ ;  $n = 35$ ).

†  $^{143}\text{Nd}/^{144}\text{Nd}$  normalized to  $^{146}\text{Sm}/^{144}\text{Nd} = 0.7219$ ; JM-Nd standard yielded  $0.511129 \pm 18$  ( $2\sigma$ , external;  $n = 42$ ) for the period January 1987 to March 1991 (samples GR100, GR102, GR103) and  $0.511125 \pm 10$  ( $2\sigma$ , external;  $n = 26$ ) for the period January 1992 to October 1993 (sample GR11). By comparison, a single analysis of the La Jolla Nd standard yields  $0.511856 \pm 6$  and no correction for interlaboratory bias is considered necessary.

‡  $^{147}\text{Sm}/^{144}\text{Nd}$  ratio determined to a precision of  $\pm 0.1\%$ .

§ Whole-rock powders repeated through dissolution, chemical separation and mass spectrometric analysis.

|| Uranium concentration determined for GR102 whole-rock iii;  $[U] = 0.080$  p.p.m.,  $^{238}\text{U}/^{204}\text{Pb} = 2.93$ .

age is  $\sim 600$  Myr older than the time of granulite metamorphism in the higher-grade part of the terrain<sup>1–6</sup> and 900 Myr older than the minerals in the adjacent trondhjemites (see below).

The initial  $\epsilon_{\text{Nd}}$  value defined by the amphibolite minerals at 3,300 Myr (see Table 2) is close to the value expected for the depleted mantle at that time (Fig. 2a). This suggests that these rocks experienced metamorphism soon after differentiation from a depleted mantle source, and were unaffected by the later granulite-facies event. By comparison, a variety of TTG lithologies in the high-grade part of this terrain experienced Sm and Nd fractionation during granulite-facies metamorphism  $\sim 2,700$  Myr ago, and preserve an initial  $\epsilon_{\text{Nd}}$  value of  $-1.89 \pm 1.58$  (combined data from refs 4, 13 and 17). The trondhjemites at Gruinard Bay define initial  $\epsilon_{\text{Nd}}$  values much lower than expected for the contemporaneous depleted mantle (Table 2), which points to a crustal source for these rocks. The evolution of the initial Nd isotope compositions from the amphibolites to the tonalites, and then to the trondhjemites, requires a  $^{147}\text{Sm}/^{144}\text{Nd}$  ratio of 0.132 (the 'best-fit' regression shown as a dashed line in Fig. 2a)—within the observed range for continental crust<sup>18,19</sup>. Thus, these data are consistent with an origin for the tonalites, and ultimately the trondhjemites, by partial melting of the older amphibolites, or similar material, formed as crust at 3,300 Myr ago. For the trondhjemites at Gruinard Bay this interpretation requires that their intrusion occurred soon before mineral equi-

libration 2,400 Myr ago. Whole-rock data for the trondhjemites give age estimates of between 2,800 and 3,000 Myr (refs 5, 12), which could be taken to indicate that intrusion occurred around that time. But if the ages reported here were to reflect final isotopic closure on the scale of the minerals, this would require that these minerals experienced complete diffusional re-equilibration of Pb and Nd isotopes, whereas the adjacent amphibolites containing similar minerals did not. Thus, the whole-rock ages are considered simply to reflect the age of the mantle source, in much the same way that the Scourie dykes have whole-rock ages of  $\sim 3,000$  Myr (ref. 20), whereas their intrusion and crystallization clearly postdates granulite formation<sup>20–22</sup>. Recent data suggest that this terrain experienced a second episode of high-grade metamorphism, and igneous intrusion,  $\sim 2,490$  Myr ago<sup>6</sup>. Metamorphism and trondhjemite emplacement at Gruinard Bay may well have occurred at this time.

In contrast to the tonalites and trondhjemites just discussed, amphibolite-facies granodiorites from the northern part of the complex<sup>12</sup> cannot have evolved in a simple manner from material having an isotopic composition like that of the amphibolites at Gruinard Bay. However, it is difficult to assess the significance of these data because of the large uncertainties associated with these results<sup>4,5,12</sup>. Moreover, some of these rocks have experienced uranium depletion<sup>5</sup>, and the same samples have unusually low Sm/Nd ratios. If the fractionation of U/Pb and Sm/Nd

TABLE 2 Mineral ages and initial isotopic compositions

	Age (Myr)		$^{143}\text{Nd}/^{144}\text{Nd}_i$	$^{206}\text{Pb}/^{204}\text{Pb}_i$	$\mu_1$	$\mu_{\text{WR}}$	$\epsilon_{\text{Nd}}^i$
	$^{206}\text{Pb}/^{207}\text{Pb}$	$^{147}\text{Sm}/^{143}\text{Nd}$					
Trondhjemitites							
GR100	$2,431 \pm 68$	$2,385 \pm 87$	$0.509346 \pm 42$	$13.530 \pm 0.088$	$7.38 \pm 0.15$	$1.43 \pm 0.22$	$-3.90 \pm 0.82$
GR103	$2,544 \pm 179$	$2,373 \pm 51$	$0.509384 \pm 28$	$13.382 \pm 0.204$	$7.46 \pm 0.37$	$0.51 \pm 0.45$	$-3.44 \pm 0.55$
Amphibolites							
GR102	$3,310 \pm 26$	$3,298 \pm 73$	$0.508549 \pm 31$	$12.186 \pm 0.030$	$8.02 \pm 0.08$	$3.18 \pm 0.07$	$+3.89 \pm 0.61$
GR11	$3,314 \pm 64$	—	—	$12,326 \pm 0.074$	$8.43 \pm 0.21$	$2.43 \pm 0.13$	—

All quoted errors are  $\pm 2\sigma$ . Definitions of quantities:  $\mu_1 = ({}^{238}\text{U}/{}^{204}\text{Pb}) = \{({}^{206}\text{Pb}/{}^{204}\text{Pb})_i - \{({}^{206}\text{Pb}/{}^{204}\text{Pb})_i\} / \exp(\lambda_{238}T - \exp(\lambda_{238}t))\}$ ;  $\mu_{\text{WR}} = ({}^{238}\text{U}/{}^{204}\text{Pb})_{\text{WR}} = \{({}^{206}\text{Pb}/{}^{204}\text{Pb})_m - \{({}^{206}\text{Pb}/{}^{204}\text{Pb})_i\} / (\exp(\lambda_{238}t) - 1)\}$ ;  $\epsilon_{\text{Nd}} = [({}^{143}\text{Nd}/{}^{144}\text{Nd})_{\text{sample}} / ({}^{143}\text{Nd}/{}^{144}\text{Nd})_{\text{CHUR}} - 1] \times 10^4$ ;  $f_{\text{Sm}/\text{Nd}} = [({}^{147}\text{Sm}/{}^{144}\text{Nd})_{\text{sample}} / ({}^{147}\text{Sm}/{}^{144}\text{Nd})_{\text{CHUR}}] - 1$ . Where  $T$  is the age of the Earth, 4,565 Myr (ref. 28);  $t$  is the  ${}^{207}\text{Pb}$ - ${}^{206}\text{Pb}$  age (given in column 1);  $\lambda_{238}$  is the decay constant for  ${}^{238}\text{U}$  (ref. 29). Subscripts 'i', 't' and 'm' indicate the initial Pb ratios at 4,565 Myr (ref. 30); the Pb ratios at time  $t$  (given in column 4) and the present-day measured Pb ratios for the whole-rock samples reported in Table 1, respectively.  $({}^{143}\text{Nd}/{}^{144}\text{Nd})_{\text{sample},i}$  is the initial  ${}^{143}\text{Nd}/{}^{144}\text{Nd}$  ratio defined by the best-fit regression line for each mineral dataset at time  $t$  (given in column 3).  $({}^{143}\text{Nd}/{}^{144}\text{Nd})_{\text{CHUR},i}$  is the  ${}^{143}\text{Nd}/{}^{144}\text{Nd}$  ratio of the chondrite uniform reservoir (CHUR)<sup>31</sup> at time  $t$ ; error propagation follows the method of Fletcher and Rosman<sup>32</sup>.

occurred after their formation, then any age or isotopic information should be interpreted with extreme caution.

The Pb isotope data can also be used to place some constraints on the behaviour of U and Pb in these rocks. The amphibolite data give model  $\mu_1$  values (the  ${}^{238}\text{U}/{}^{204}\text{Pb}$  ratio which describes evolution in the source rocks from 4,565 Myr to the determined age, see Table 2) close to recent estimates for the depleted mantle<sup>23,24</sup>. A second  $\mu$  value may be calculated from the whole-rock data: this model  $\mu_{\text{WR}}$  reflects the  ${}^{238}\text{U}/{}^{204}\text{Pb}$  ratio for the sample from its formation time to the present day. Values of  $\mu_{\text{WR}}$  for the trondhjemitites are low (Table 2), which may either be attributed to uranium depletion during metamorphism, or may reflect the low  $\mu$  of their source. However, the  $\mu_{\text{WR}}$  values of 3.18 and 2.43 for the amphibolites are also low (Table 2), in good agreement with the present day  ${}^{238}\text{U}/{}^{204}\text{Pb}$  ratio of 2.93

measured for sample GR102 (see Table 1 legend). This may indicate that the amphibolites also experienced a reduction in their U/Pb ratio during metamorphism 3,300 Myr ago. Alternatively, this may be due to the magmatic processes responsible for the generation of the precursors of the amphibolites, during which the source  $\mu$  of  $\sim 8.2$  was reduced to a value of  $\sim 3$ . In either case, if the tonalites and the trondhjemitites were indeed produced by partial melting of this older amphibolite crust then their  $\mu_1$  values should preserve some evidence of a crustal pre-history, from 3,300 Myr to their determined age, with a low  $\mu$  of  $\sim 3$ . Figure 2b indicates that the  $\mu_1$  values for the amphibolites, tonalites and trondhjemitites with ages ranging from 3,300 to 2,400 Myr may be related. If it is assumed that the dashed line shown in Fig. 2b reflects the Pb evolution in a lithospheric source over this time interval, then the particular  $\mu$  value for that source

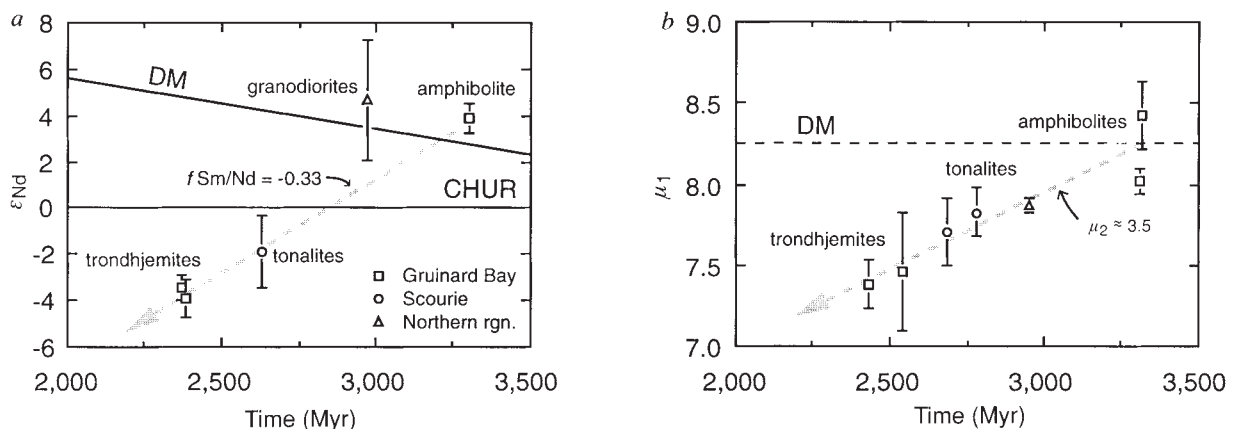


FIG. 2 a, Plot of initial  $\epsilon_{\text{Nd}}$  against time (Myr ago) for the amphibolite and trondhjemitite minerals from Gruinard Bay (squares), for the granulite-facies TTG lithologies (circles) at Scourie<sup>4,13,17</sup>, and amphibolite-facies granodiorites (triangle) from the northern part of the Lewisian complex<sup>12</sup>. All data are expressed relative to the chondrite uniform reservoir (CHUR)<sup>31</sup>, defined as  $\epsilon_{\text{Nd}} = 0$ . Also shown is the model depleted-mantle (DM) evolution curve of Goldstein *et al.*<sup>19</sup>. The initial  $\epsilon_{\text{Nd}}$  value for the amphibolite minerals is close to that expected for the depleted mantle at that time (see text). The apparent evolution of  $\epsilon_{\text{Nd}}$  values from the amphibolites to the tonalites, and then to the trondhjemitites (the best-fit regression shown as a dashed line) requires an  $f_{\text{Sm}/\text{Nd}}$  value of  $-0.33$  (where  $f_{\text{Sm}/\text{Nd}}$  is the Sm/Nd ratio relative to CHUR; see Table 2 legend)—within the range of values for the continental crust<sup>18,19</sup>. Note, however, that the amphibolite-facies granodiorites from the northern region do not fall on the line, and therefore cannot have evolved in this simple manner (see text). These data suggest that many of the TTG lithologies in the Lewisian may have been formed by partial melting of the older amphibolitic crust, or similar material, preserved at Gruinard Bay. b, Comparison of  $\mu_1$  values ( ${}^{238}\text{U}/{}^{204}\text{Pb}$  ratios which describe Pb isotope evolution from 4,565 Myr to time  $t$ ) against time (Myr ago) for

the amphibolite and trondhjemitite minerals from Gruinard Bay, and the whole-rock tonalite data from Scourie and the northern region (data from refs 3–5). The amphibolites from Gruinard Bay give  $\mu_1$  values close to a recent estimate of  $8.26 \pm 0.1$  for the depleted mantle<sup>24</sup>, shown as a dashed line (labelled DM). At 3,300 Myr the source  $\mu$  of the amphibolites was reduced to a value of  $\sim 3$  (see Table 2). If the variation of  $\mu_1$  values with time in the TTG lithologies is related to the development of a single lithospheric source region, then its characteristic  ${}^{238}\text{U}/{}^{204}\text{Pb}$  ( $\mu_2$ ) value for the time interval 3,300 to 2,400 Myr is defined from the slope of the best-fit regression, shown as a dashed line. The best estimate is  $\mu_2 \approx 3.5$ . Thus, these data suggest that the TTG lithologies may have been derived from a lithospheric source with a low  $\mu$ , similar to that of the amphibolites. (Definitions of quantities:  $\mu_2 = (\mu^* \exp(\lambda_{238}T) - 1) / ((\mu_1 \exp(\lambda_{238}T) - 1) / (\exp(\lambda_{238}t_1) - 1))$ , where  $\mu_1$  is the  $\mu$  value from 4,565 Myr to  $t_1$  (3,300 Myr),  $\mu^*$  is the  $\mu$  value from 4,565 Myr to  $t_2$  (the time of Pb isotope equilibration,  $\mu_2$  is the  $\mu$  value from  $t_1$  (3,300 Myr) to  $t_2$ ,  $T$  is the age of the Earth, 4,565 Myr (ref. 28) and  $\lambda_{238}$  is the decay constant for  ${}^{238}\text{U}$  (ref. 29). From the best-fit line shown when  $t = 3,300$  Myr,  $\mu_1 = \mu^* = 8.23$ ; when  $t = 0$ ,  $\mu^* = \text{intercept} = 5.13$ .)



is calculated to be  $\mu_2 \approx 3.5$  (see Fig. 2b legend). This result gives no constraint on the time of formation of the TTG rock types, but simply indicates that they may have been derived from a lithospheric source with a low  $\mu$ , similar to that of the amphibolites at Gruinard Bay. Many granulites show extreme depletion in uranium<sup>25,26</sup>, which gives rise to very low  $\mu$  values. But in the present case the low  $\mu$  values must have developed, at least in part, before granulite-facies metamorphism and are related either to magmatic processes<sup>27</sup> or to lower-grade amphibolite-facies metamorphism<sup>1</sup> rather than to granulite formation itself.

The Lewisian complex, like many Archaean terrains and hence the bulk of the early continental crust, is dominated by TTG rock types. Consequently, understanding the melting processes responsible for their generation, and the timescale over which this occurs, are central to ideas on early continent formation. Petrogenic and trace-element constraints suggest that these rocks are formed by partial melting of pre-existing mafic crust<sup>7-11</sup>. But before this work, potential source material had eluded detection and the Lewisian TTG rock types were considered to have formed within ~300 Myr of granulite metamorphism at ~2,700 Myr. Our results indicate that the amphibolites at Gruinard Bay have been in existence for at least 3,300 Myr, and thus the Lewisian TTG rocks may have developed over a much longer time interval than previously assumed. The amphibolites possess initial isotopic compositions close to those anticipated for the depleted mantle at that time. Furthermore, the apparent evolution of Nd and Pb isotopes within many of the TTG lithologies in the Lewisian suggests that they may have been derived from a pre-existing lithospheric source, with an isotopic signature similar to that of the amphibolites at Gruinard Bay. It seems possible that multiple stages of lithospheric processing, such as described here, may characterize the development of TTG rocks, both in the Lewisian complex and in other Archaean terrains. Under these circumstances only the earliest remnants in such terrains are likely to preserve information on the isotopic composition of contemporary depleted mantle. □

Received 29 June; accepted 5 July 1994.

1. Moorbath, S., Welke, H. & Gale, N. H. *Earth planet. Sci. Lett.* **6**, 245-256 (1969).
2. Pidgeon, R. T. & Bowes, D. R. *Geol. Mag.* **109**, 247-258 (1972).
3. Chapman, H. J. & Moorbath, S. *Nature* **268**, 41-42 (1977).
4. Whitehouse, M. J. *Nature* **331**, 705-707 (1988).
5. Whitehouse, M. J. *Geochim. cosmochim. Acta* **53**, 717-724 (1989).
6. Corfu, F., Heaman, L. M. & Rogers, G. *Contr. Miner. Petrol.* (in the press).
7. Arth, J. G. & Hanson, G. N. *Contr. Miner. Petrol.* **37**, 161-174 (1972).
8. Arth, J. G. & Barker, F. *Geology* **4**, 534-536 (1976).
9. Rollinson, H. R. & Windley, B. F. *Contr. Miner. Petrol.* **72**, 265-281 (1980).
10. Weaver, B. L. & Tarney, J. *Earth planet. Sci. Lett.* **51**, 279-296 (1980).
11. Martin, H. *Geology* **14**, 753-756 (1986).
12. Whitehouse, M. J. *Tectonophysics* **161**, 245-256 (1989).
13. Cohen, A. S., O'Nions, R. K. & O'Hara, M. J. *Contr. Miner. Petrol.* **106**, 142-153 (1991).
14. Rollinson, H. R. & Fowler, M. B. in *Evolution of the Lewisian and Comparable Precambrian High Grade Terrains* (eds Park, R. G. & Tarney, J.) 57-71 (Spec. Publ. No. 27, Geol. Soc. Lond. 1987).
15. Rollinson, H. R. *Mineralog. Mag.* **51**, 345-355 (1987).
16. Burton, K. W. & O'Nions, R. K. *Earth planet. Sci. Lett.* **107**, 649-671 (1991).
17. Hamilton, P. J., Evensen, N. M., O'Nions, R. K. & Tarney, J. *Nature* **277**, 25-28 (1979).
18. Taylor, S. R. & McLennan, S. M. *The Continental Crust: Its Composition and Evolution* (Blackwell, Oxford, 1985).
19. Goldstein, S. L., O'Nions, R. K. & Hamilton, P. J. *Earth planet. Sci. Lett.* **70**, 221-236 (1984).
20. Waters, F. G., Cohen, A. S., O'Nions, R. K. & O'Hara, M. J. *Earth planet. Sci. Lett.* **97**, 241-255 (1990).
21. Chapman, H. J. *Nature* **277**, 642-643 (1979).
22. Heaman, L. M. & Tarney, J. *Nature* **340**, 705-708 (1989).
23. White, W. M. *Earth planet. Sci. Lett.* **115**, 211-226 (1993).
24. Asmerom, V. & Jacobsen, S. B. *Earth planet. Sci. Lett.* **115**, 245-256 (1993).
25. Heier, K. S. *Phil. Trans. R. Soc. A273*, 429-442 (1973).
26. Rudnick, R. L. & Presper, T. in *Granulites and Crustal Evolution* (eds Vielzeuf, D. & Vidal, P.) 523-550 (Kluwer, Amsterdam, 1990).
27. Tarney, J. & Weaver, B. L. in *Evolution of the Lewisian and Comparable Precambrian High Grade Terrains* (eds Park, R. G. & Tarney, J.) 45-56 (Spec. Publ. No. 27, Geol. Soc. Lond. 1987).
28. Göpel, C., Manhès, G. & Allègre, C. J. *Earth planet. Sci. Lett.* **121**, 153-171 (1994).
29. Steiger, R. H. & Jäger, E. *Earth planet. Sci. Lett.* **36**, 359-362 (1977).
30. Tatsumoto, M., Knight, R. J. & Allègre, C. J. *Science* **180**, 1279-1283 (1973).
31. Jacobsen, S. B. & Wasserburg, G. J. *Earth planet. Sci. Lett.* **50**, 139-155 (1980).
32. Fletcher, I. R. & Rosman, K. J. R. *Geochim. cosmochim. Acta* **46**, 1983-1987 (1982).

ACKNOWLEDGEMENTS. We thank H. J. Chapman, M. J. Bickle and M. J. Whitehouse for their thoughtful and constructive comments on this work, and S. J. G. Galer for insight into the U/Pb systematics. This research was supported by the UK NERC and the Royal Society.

## Processing of tumour necrosis factor- $\alpha$ precursor by metalloproteinases

A. J. H. Gearing, P. Beckett, M. Christodoulou, M. Churchill, J. Clements, A. H. Davidson, A. H. Drummond, W. A. Galloway, R. Gilbert, J. L. Gordon\*, T. M. Leber, M. Mangan, K. Miller, P. Nayee, K. Owen, S. Patel, W. Thomas, G. Wells, L. M. Wood & K. Woolley

British Biotech, Watlington Road, Cowley, Oxford OX4 5LY, UK

TUMOUR necrosis factor- $\alpha$  (TNF- $\alpha$ ) is a potent pro-inflammatory and immunomodulatory cytokine implicated in inflammatory conditions such as rheumatoid arthritis, Crohn's disease, multiple sclerosis and the cachexia associated with cancer or human immunodeficiency virus infection<sup>1</sup>. TNF- $\alpha$  is initially expressed as a 233-amino-acid membrane-anchored precursor which is proteolytically processed to yield the mature, 157-amino-acid cytokine<sup>2</sup>. The processing enzyme(s) which cleave TNF- $\alpha$  are unknown. Here we show that the release of mature TNF- $\alpha$  from leukocytes cultured *in vitro* is specifically prevented by synthetic hydroxamic acid-based metalloproteinase inhibitors, which also prevent the release of TNF- $\alpha$  into the circulation of endotoxin challenged rats. A recombinant, truncated TNF- $\alpha$  precursor is cleaved to biologically active, mature TNF- $\alpha$  by several matrix metalloproteinase enzymes. These results indicate that processing of the TNF- $\alpha$  precursor is dependent on at least one matrix metalloproteinase-like enzyme, inhibition of which represents a novel therapeutic mechanism for interfering with TNF- $\alpha$  production.

Examination of the sequences surrounding the proposed cleavage site of the TNF- $\alpha$  precursor revealed homologies with peptide sequences known to be cleaved by matrix metalloproteinases (MMPs). We therefore tested the effects of several synthetic hydroxamic acid-based inhibitors of MMPs on the release of TNF- $\alpha$ . A number of these inhibitors prevented TNF- $\alpha$  production, whereas diastereoisomers, inactive against MMPs, did not. In an assay of TNF- $\alpha$  release from endotoxin-stimulated human blood cultures, BB-2284, BB-2275 and BB-2116 had IC<sub>50</sub> values (50% inhibitory concentrations) of 400, 580 and 230 nM respectively. This is approximately 100-fold more potent than pentoxifylline (see Fig. 1), which inhibits TNF- $\alpha$  production at the genetic level and is used in the clinic to treat diseases in which TNF- $\alpha$  is known to be involved<sup>3</sup>. Inhibitors of non-matrix metalloproteinases such as angiotensin converting enzyme, enkephalinase and endothelin converting enzyme<sup>4,5</sup> had no effect on TNF- $\alpha$  production (Fig. 1), and inhibitors of serine proteases (aprotinin, 10  $\mu$ M; elastinal, 200  $\mu$ M), serine/cysteine proteases (leupeptin, 100  $\mu$ M), cysteine proteases (E64, 100  $\mu$ M), aspartyl proteases (pepstatin, 100  $\mu$ M) and aminopeptidase (Bestatin, 100  $\mu$ M)<sup>6</sup> were also ineffective. The effect of BB-2284 was specific for TNF- $\alpha$  processing: no significant inhibition of the release of the interleukins IL-1 $\beta$ , IL-6, IL-8 and IL-10, G-CSF or GM-CSF from whole blood cultures was observed (results for TNF- $\alpha$ , IL-1 $\beta$  and IL-8 are shown in Fig. 2a-c).

To establish whether the processing of pro-TNF- $\alpha$  by a metalloproteinase was direct or indirect we used a recombinant glutathione-S-transferase-linked pro-TNF- $\alpha$  fusion protein (GST-TNF- $\alpha$ ) as a substrate. This was recognized by several antibodies to TNF- $\alpha$  and was biologically active in an L-929 cytotoxicity assay<sup>7</sup>. Addition of MMPs such as PUMP (matrilysin; MMP-7), stromelysin-1 (MMP-3), collagenase (MMP-1),

\* To whom correspondence should be addressed, at: NEURES Ltd, 4-10 The Quadrant, Barton Lane, Abingdon, Oxon OX14 3YS, UK.